European Journal of Medicinal Chemistry 44 (2009) 4393–4403

Contents lists available at ScienceDirect

European Journal of Medicinal Chemistry

journal homepage: http://www.elsevier.com/locate/ejmech

Original article

Synthesis, crystal structures and antibacterial activity studies of aza-derivatives of phytoalexin from cotton plant – gossypol

Piotr Przybylski [a,*], Krystian Pyta [a], Joanna Stefańska [b], Małgorzata Ratajczak-Sitarz [a], Andrzej Katrusiak [a], Adam Huczyński [a], Bogumil Brzezinski [a]

[a] Faculty of Chemistry, A. Mickiewicz University, Grunwaldzka 6, 60-780 Poznan, Poland
[b] Medical University, Department of Pharmaceutical Microbiology, Oczki 3, 02-007 Warsaw, Poland

ARTICLE INFO

Article history:
Received 15 January 2009
Accepted 31 May 2009
Available online 12 June 2009

Keywords:
Gossypol aza-derivatives
Antibacterial activity
Tautomerism
X-ray
Spectroscopy

ABSTRACT

Using Gossypol (GOS) extracted from cotton seeds, a series of its Schiff bases (**1**–**18**) and hydrazones (**19**–**27**) have been synthesized and evaluated for their antimicrobial activities against Gram-positive bacteria, Gram-negative bacteria and yeast-like organisms. Of the 27 aza-derivatives of gossypol, 11 have been found active against the microorganisms tested, similar to gossypol. Crystal structures of the new Schiff base (compound **7**) and hydrazone (compound **25**) of gossypol reveal the presence of two different tautomers within two types of the aza-derivatives studied. The newly synthesized aza-derivatives of gossypol are characterized by the FT-IR, NMR and MS methods.

1. Introduction

Gossypol (Scheme 1), bissesquiterpene from cotton seeds [1], is mainly known as prospective component of contraceptive pill for man [2]. Furthermore, this compound is characterized by wide antiviral [3–6], anticancer [7–9] and antifungal [10,11] properties. However, the relatively high toxicity of gossypol [12], evoked by the presence of two aldehyde groups, precludes its application in medical therapy. For this reason the syntheses and tests of gossypol derivatives, in which both aldehyde groups are blocked, are desired to enable their application as drugs. Up to now many gossypol derivatives including its Schiff bases, periacetylated gossylic nitriles, periacetylated gossylic imino-lactones, azo-derivatives, hydrazones, thioderivatives of gossypol have been obtained [13–19] and tested for their antipsoriatic [20], antimalarial [21], anticancer [22,23], interferon-inducing [24] as well as anti-HIV [25] activity. Earlier studies have shown that the activity of gossypol is rather bacteriostatic than antibacterial [26–28] although gossypol structural analogues like hemigossypol, 2,7-dihydroxycadalene, lacinilene and their respective 7-methyl esters have shown very promising antibacterial activity [29,30]. The limited antibacterial activity of gossypol can be probably concerned with the relatively poor ability to form complexes with the monovalent cations such as Na^+ or K^+ [31]. In our earlier papers we have reported the synthesis and the physicochemical properties of some Schiff bases or hydrazones of gossypol [14,19,32,33]. The complexation of biologically important monovalent metal cations such as Na^+ and K^+, by aza-derivatives of gossypol has been proved and described in detail [34,35]. Up to now, however, no antibacterial activity studies of the Schiff bases or hydrazones of gossypol have been performed. Dao et al. suggested that the cytotoxicity of gossypol derivatives depends on the availability of the phenolic oxygen atoms of gossypol derivatives [36]. The aza-derivatives of gossypol in the solution can be present in the various tautomeric forms (Scheme 1) which differ from each other by the number of phenolic groups [33,37,38]. Taking into account the enormous number of Schiff bases of gossypol synthesized, only several of them have been studied by the X-ray methods [31,39–43]. No crystal structures of any gossypol hydrazones have been reported till now despite the fact that many crystal structures of other groups of hydrazones, e.g. hydrazones containing heterocyclic moieties are well known [44]. In this paper the structures of a new Schiff base and new hydrazone of gossypol (**7** and **25**) are reported. The main aim of the paper is the discussion of the relationship between antibacterial activity and the structure of the gossypol Schiff bases and hydrazones (Scheme 2) with substituents of different bulk and polarity.

* Corresponding author. Tel.: +48 61 8291252; fax: +48 61 829 1505.
E-mail address: piotrp@amu.edu.pl (P. Przybylski).

0223-5234/$ – see front matter © 2009 Elsevier Masson SAS. All rights reserved.
doi:10.1016/j.ejmech.2009.05.032

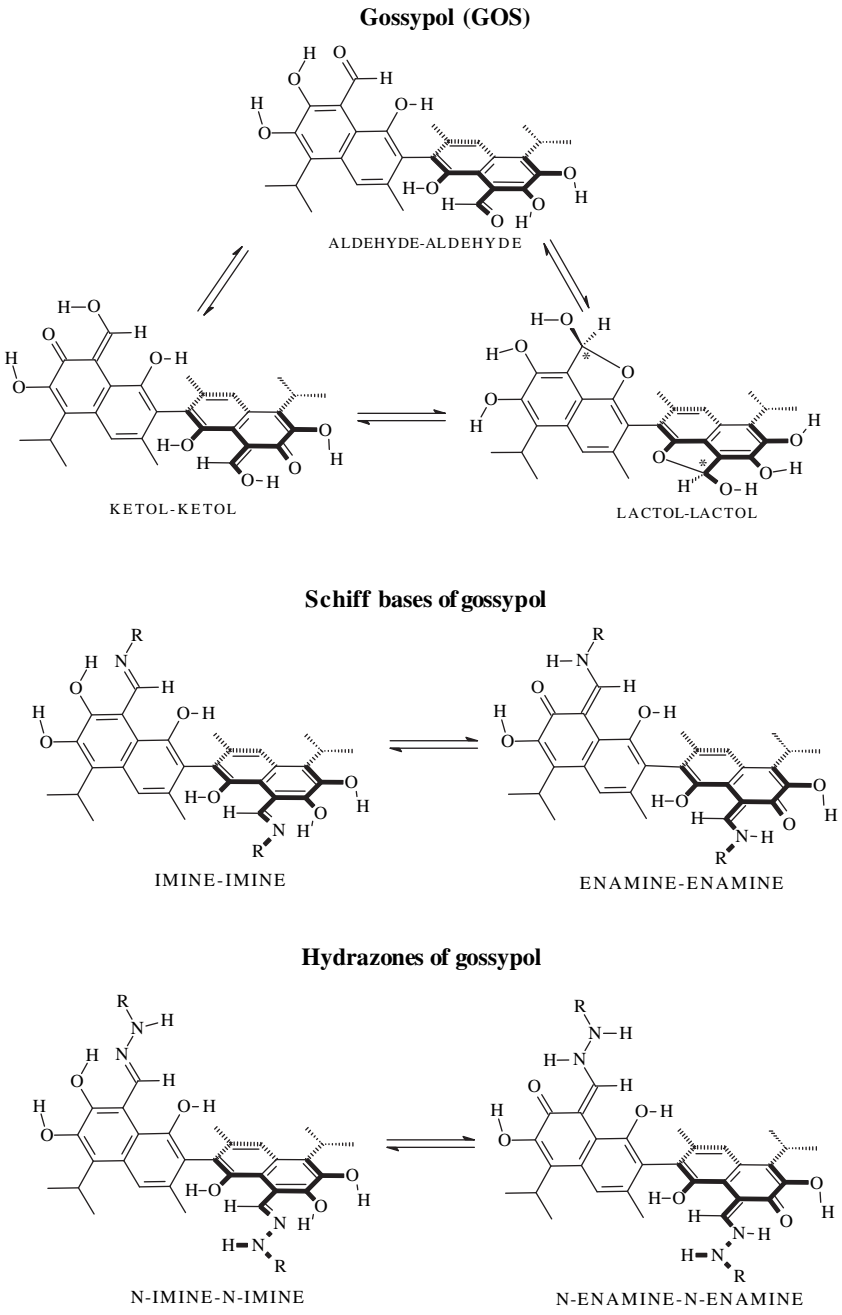

Scheme 1. Tautomeric forms of gossypol and its aza-derivatives.

2. Chemistry

2.1. X-ray studies

The atom numbering applied for X-ray studies is given in Figs. 1 and 2. The crystal structures of compounds **7** and **25** differ significantly in symmetry, molecular arrangement and molecular structure (Table 1). The main difference in the molecular structure is associated with the proton position in the intramolecular O(2)···H···N(16) hydrogen bridges (Figs. 1 and 2). In **7** the proton resides at N(16) while in **25** it resides at O(2). This result indicates that in the solid state within the structures of **7** and **25** two different tautomeric forms, i.e. the enamine–enamine and N-imine–N-imine are realized, respectively. Despite the proton positions in the intramolecular hydrogen bonds the length of these bonds are comparable (Tables 3 and 4). Furthermore, the values of the C–O, C–N and C–C bond lengths (Table 2) demonstrate that the intramolecular hydrogen bonds formed within the two different tautomers are assisted by the resonance within the π electron aromatic system [45–48]. Significant difference in the C(7)–O(2) bond lengths in the crystal structures of **7** and **25** indicates clearly that the former structure includes – a carbonyl group, whereas the latter structure – a hydroxyl group in the naphthalene rings. The parameters of the intramolecular hydrogen bonds in the two parts of Schiff base molecule (**7**) are more similar than those in the analogues two parts of the hydrazone molecule (**25**) (Tables 3 and 4). In the structure of **25** the distortion in symmetry is related to the various conformations of the piperazine rings within the two parts

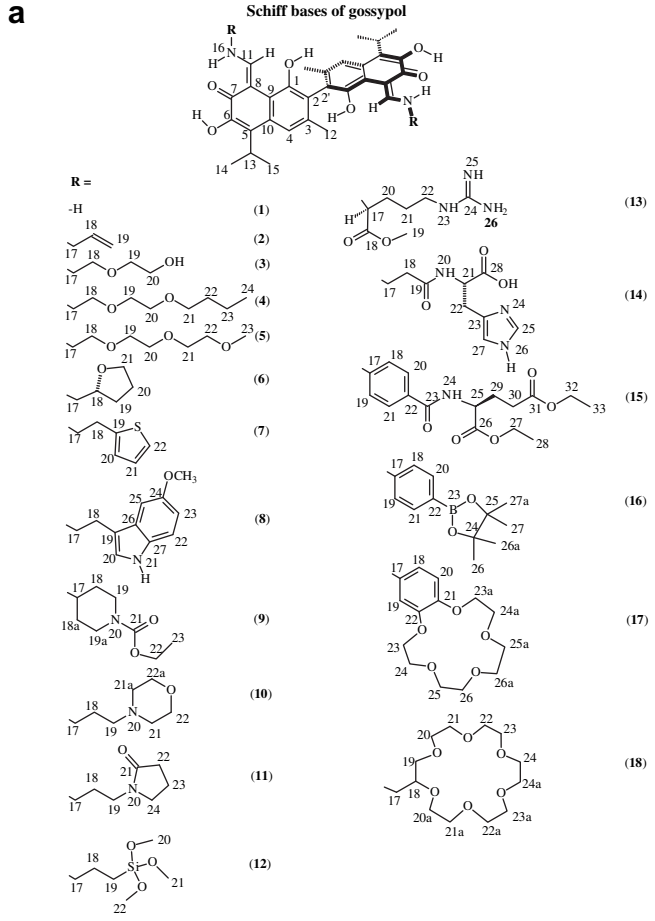

Scheme 2. Chemical structure and atom numbering (applied for spectroscopic studies) of gossypol and its Schiff bases and hydrazones.

of the molecule as well as to the involvement of N(22) and N(22′) nitrogen atoms of the piperazine rings in the intermolecular hydrogen bonds of different strength and geometry. This is also the reason for different availability of the electron lone pairs at the N(17) and N(17′) atoms in the resonance of the π electron system, which is reflected in different N(16)–N(17) and N(16′)–N(17′) bond lengths.

Table 1
Crystal data and structure refinement for **7** and **25** derivatives.

Compound	**7**	**25**
Empirical formula	$C_{42}H_{44}N_2O_6S_2$	$C_{40}H_{52}N_6O_6$
Formula weight	736.91	712.88
Temperature (K)	293(2)	293(2)
Wavelength	0.71073 Å	0.71073 Å
Crystal system, space group	Triclinic, *P*-1	Orthorhombic, *Pccn*
Unit cell dimensions	$a = 10.7717(5)$ Å $b = 14.2310(5)$ Å $c = 15.0623(7)$ Å	$a = 34.934(9)$ Å $b = 16.025(3)$ Å $c = 14.917(3)$ Å
Angles	$\alpha = 112.031(4)^\circ$ $\beta = 104.377(4)^\circ$ $\gamma = 101.687(3)^\circ$	$\alpha = 90^\circ$ $\beta = 90^\circ$ $\gamma = 90^\circ$
Volume	1957.66(15) Å^3	8350(3) Å^3
Z	2	8
Calculated density	1.250 g cm^{-3}	1.134 g cm^{-3}
Absorption coefficient	0.185 mm^{-1}	0.077 mm^{-1}
F(000)	780	3056
Crystal size	0.35 × 0.15 × 0.125 mm	0.25 × 0.10 × 0.075 mm
θ range for data collection	2.10–29.68°	2.20–22.50°
Limiting indices	$-14 \le h \le 11$, $-18 \le k \le 19$, $-19 \le l \le 20$	$-36 \le h \le 37$, $-17 \le k \le 17$, $-16 \le l \le 9$
Reflections collected/unique	23,491/9708, $R_{int} = 0.0984$	50,164/5459, $R_{int} = 0.5645$
Completeness	to $\theta = 29.68$, 87.6%	to $\theta = 29.85$, 99.9%
Refinement method	Full-matrix least-squares on F^2	Full-matrix least-squares on F^2
Data/restraints/parameters	9708/0/468	5459/1/474
Goodness-of-fit on F^2	0.998	0.681
Final *R* indices $[I > 2\sigma(I)]$	$R_1 = 0.0787$, $wR_2 = 0.1719$	$R_1 = 0.0694$, $wR_2 = 0.1238$
R indices (all data)	$R_1 = 0.3233$, $wR_2 = 0.2123$	$R_1 = 0.3880$, $wR_2 = 0.1815$
Largest diff. peak and hole	0.537 and −0.506 e Å^{-3}	0.213 and −0.183 e Å^{-3}

Table 2
Comparison of selected bond lengths (Å) and angles (°) in the X-ray structures of **7** and **25**.

Bond length (Å)	**7**	**7′**	**25**	**25′**
O(1)–C(1)	1.374(5)	1.379(5)	1.396(9)	1.341(11)
O(2)–C(7)	1.295(5)	1.293(5)	1.334(12)	1.393(10)
O(3)–C(6)	1.376(5)	1.381(5)	1.428(12)	1.446(15)
C(2)–C(2′)	1.497(6)	–	1.461(12)	–
C(8)–C(11)	1.416(6)	1.406(6)	1.470(11)	1.457(13)
C(11)–N(16)	1.312(5)	1.304(6)	1.276(9)	1.322(10)
C(5)–C(6)	1.346(6)	1.353(6)	1.328(11)	1.287(17)
C(6)–C(7)	1.434(6)	1.440(6)	1.359(13)	1.426(15)
C(7)–C(8)	1.420(5)	1.429(6)	1.390(12)	1.369(13)
N(16)–N(17)	–	–	1.382(10)	1.462(10)
Bond angle (°)	**7**	**7′**	**25**	**25′**
H(3)–O(3)–O(6)	109.5	109.5	94.8	93.8
C(5)–C(6)–O(3)	121.4(5)	121.0(4)	116.4(14)	125.3(15)
C(5)–C(6)–C(7)	124.8(5)	124.7(5)	125.0(14)	126.3(17)
O(3)–C(6)–C(7)	113.8(4)	114.2(5)	118.3(13)	108.3(17)
O(2)–C(7)–C(8)	124.5(5)	124.6(5)	123.6(13)	118.8(15)
O(2)–C(7)–C(6)	116.1(4)	117.6(5)	114.4(15)	119.1(15)
C(8)–C(7)–C(6)	119.4(5)	117.7(5)	122.0(13)	122.1(13)
C(11)–C(8)–C(7)	117.2(4)	117.0(5)	117.1(12)	120.8(15)
C(11)–C(8)–C(9)	124.0(4)	123.9(4)	128.3(13)	123.0(13)
C(7)–C(8)–C(9)	118.7(4)	119.0(4)	114.5(12)	116.2(13)
N(16)–C(11)–C(8)	122.4(5)	126.0(5)	120.0(11)	120.3(12)
C(11)–N(16)–H(16)	110(3)	109(3)	–	–
C(7)–O(2)–H(2)	–	–	103.0	109.4
C(1)–C(2)–C(2′)–C(1′)	97.2(5)	–	107.9(13)	–
C(9)–C(8)–C(11)–N(16)	179.9(4)	179.0(5)	−175.4(10)	166.8(11)
C(10)–C(5)–C(13)–C(15)	−93.6(6)	−121.7(6)	−130.1(10)	106(2)
C(10)–C(5)–C(13)–C(14)	138.1(5)	103.4(6)	106.1(11)	−115.5(17)

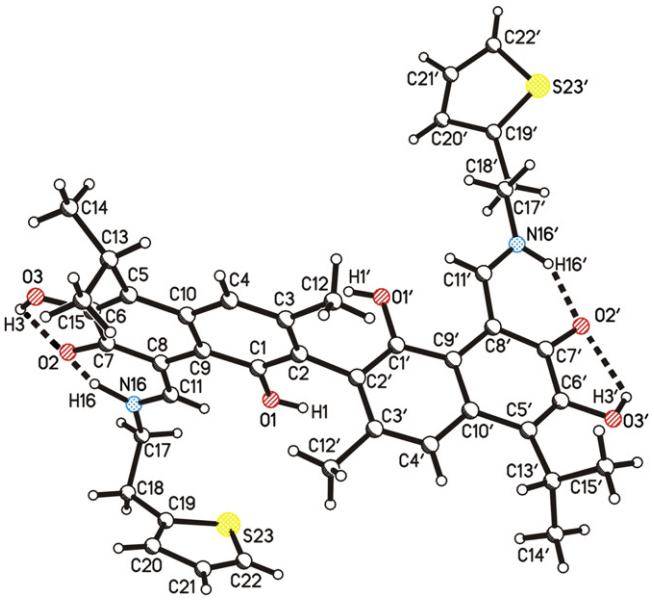

Fig. 1. A perspective view of **7** in the crystal structure. Intramolecular hydrogen bonds have been indicated by dashed lines.

Furthermore, in **7** only O(1′)–H and not O(1)–H group is involved in a relatively short intermolecular hydrogen bond to O(2) carbonyl group of the molecule transformed *via* an inversion center. The intermolecular O(1′)–H···O(2)=C(7) hydrogen bond links the molecules into helixes along the [100] direction (Table 3). In both crystals the sesquiterpene systems are only slightly stacked, as illustrated in Figs. 3 and 4.

2.2. FT-IR studies

The atom numbering applied for FT-IR and NMR spectroscopic studies is given in Scheme 2. The exemplary FT-IR spectra of **7** and **25** and for comparison the spectrum of gossypol in the KBr pellets, are compared in Fig. 5a.

Table 3
Dimensions of the hydrogen bonds (Å and °) within gossypol Schiff base (**7**) crystal structure.

D–H···A	*d*(D–H)	*d*(H···A)	*d*(D···A)	∠(DHA)
O(3)–H(3)···O(2)	0.82	2.07	2.560(5)	118
O(3′)–H(3′)···O(2′)	0.82	2.13	2.607(4)	117
N(16)–H(16)···O(2)	1.16(6)	1.50(6)	2.516(5)	142
N(16′)–H(16′)···O(2′)	0.93(4)	1.78(5)	2.597(5)	145
O(1′)–H(1′)···O(2)^{i}	0.82	2.00	2.635(4)	134
O(3′)–H(3′)···O(2′)^{ii}	0.82	2.46	3.126(5)	139
O(3)–H(3)···S(23)^{iii}	0.82	3.13	3.223(4)	89

Symmetry codes: (i): $1-x, 1-y, 1-z$; (ii): $3-x, 1-y, 2-z$; (iii): $x-1, y, z$.

Table 4
Dimensions of the hydrogen bonds (Å and °) within gossypol hydrazone (**25**) crystal structure.

D–H···A	*d*(D–H)	*d*(H···A)	*d*(D···A)	∠(DHA)
O(2)–H(2)···N(16)	0.77	1.802	2.458(12)	143
O(2′)–H(2′A)···N(16′)	0.82	1.725	2.474(12)	151
O(3)–H(3)···O(2)	1.00	1.866	2.589(10)	126
O(3′)–H(3′A)···O(2′)	0.85	1.904	2.568(9)	134
O(1)–H(1A)···N(22′)^{i}	0.82	2.341	2.966(11)	134
O(1′)–H(1′)···N(22)^{ii}	1.11	1.868	2.827(11)	142

Symmetry codes: (i): $x, 0.5-y, 0.5+z$; (ii): $x, 0.5-y, -0.5+z$.

The same spectra with extended scale representing the region of the ν(C=O, C=N) stretching vibrations are shown in Fig. 5b.

The spectra of **7** and **25** (Fig. 5a, blue and red lines, respectively) show two bands assigned to the ν(OH) vibrations at ca. 3484 and 3307 cm^{-1}. According to X-ray results, the position of the band at higher wavenumbers indicates very weak intramolecular interactions of the OH groups at position 1 with the π electron system, whereas the other band suggests that the hydrogen-bonded OH groups at positions 1′ and 6,6′ form slightly stronger inter- and intramolecular hydrogen bonds. The proton vibrations of the strongest hydrogen-bonded proton in the intramolecular O···H···N hydrogen bond should be observed in the FT-IR spectra in the region below 3000 cm^{-1}. This absorption is, however, not well visible in the respective spectra taken for solids. This observation

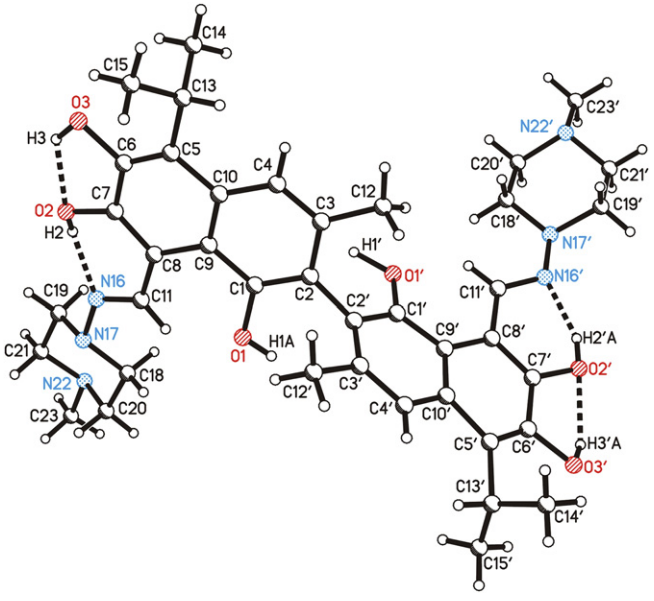

Fig. 2. A perspective view of **25** in the crystal structure. Intramolecular hydrogen bonds have been indicated by dashed lines.

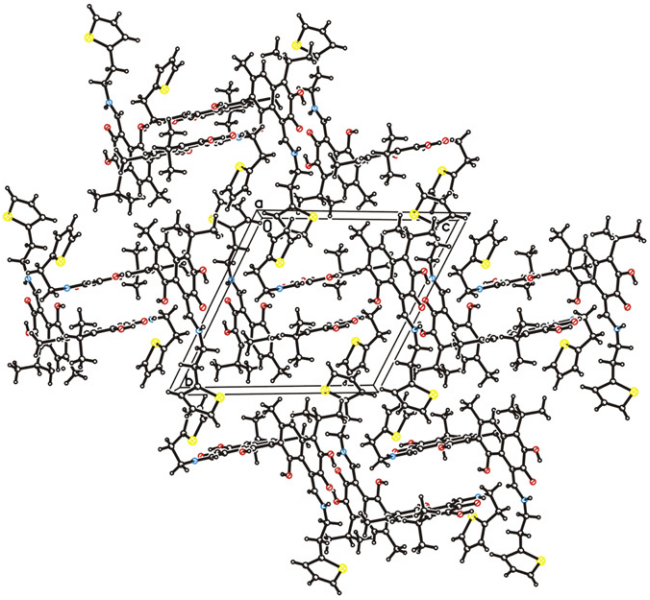

Fig. 3. Arrangement of **7** in the crystal lattice, projected along the [100] direction.

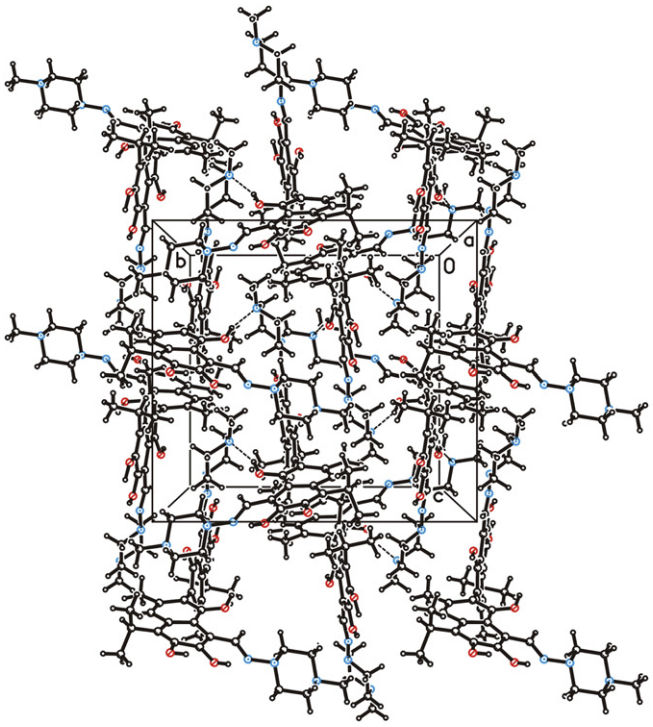

Fig. 4. Arrangement of **25** in the crystal lattice, projected along the [100] direction.

can be explained by a strong coupling of the motion of the protons engaged in the intramolecular hydrogen bond with π electrons, resulting in the vanishing of the proton polarizability [49,50]. In the spectrum of **25** the presence of the two so-called Bohlmann bands [51–53] at 2811 and 2848 cm^{-1} proves the occurrence of N atoms within the structure, at which the lone electron pairs are localized. According to the X-ray data the Bohlmann bands can be assigned to the vibrations of the lone electron pairs at N(17) and N(17′) atoms.

The most important spectroscopic details concerning the structures of **7** and **25** are obtained from the spectra in the region 1750–1500 cm^{-1} (Fig. 5b). In the spectrum of **7**, the bands assigned to the $\nu(C_7{=}O)$ and $\nu(C_8{=}C_{11})$ vibrations arise as one broad band being a superposition of two bands with maxima at about 1629 cm^{-1} and 1619 cm^{-1} indicating the formation of the enamine–enamine form within the structure of the Schiff base. Furthermore, the formation of enamine–enamine form is also confirmed by very strong changes in the band assigned to the ν(C=C) vibrations, characteristic of naphthalene ring. In the spectrum of GOS, the band assigned to these vibrations is found at 1573 cm^{-1}, whereas in the spectrum of **7**, this band vanishes and new bands arise at about 1528 and 1513 cm^{-1}.

In the spectrum of **25**, the band assigned to the $\nu(C_{11}{=}O)$ aldehyde vibration observed in the spectrum of gossypol at 1622 cm^{-1} vanishes completely and, in contrast to the spectrum of **7**, only one broad band at about 1608 cm^{-1} appears, caused mainly by the overlaying of the bands assigned to the $\nu(C_{11}{=}N)$ and ν(C=C) vibrations. This spectral feature clearly indicates the formation of the N-imine–N-imine tautomeric form (analogous to the aldehyde–aldehyde form of gossypol) within the **25** molecule.

2.3. NMR studies

The formulae of compounds **1**–**27** studied and the carbon atoms numbering are shown in Scheme 2. The most important ^{1}H and ^{13}C NMR data of **1**–**27** and of gossypol for comparison in three various solvents are shown in Table 5.

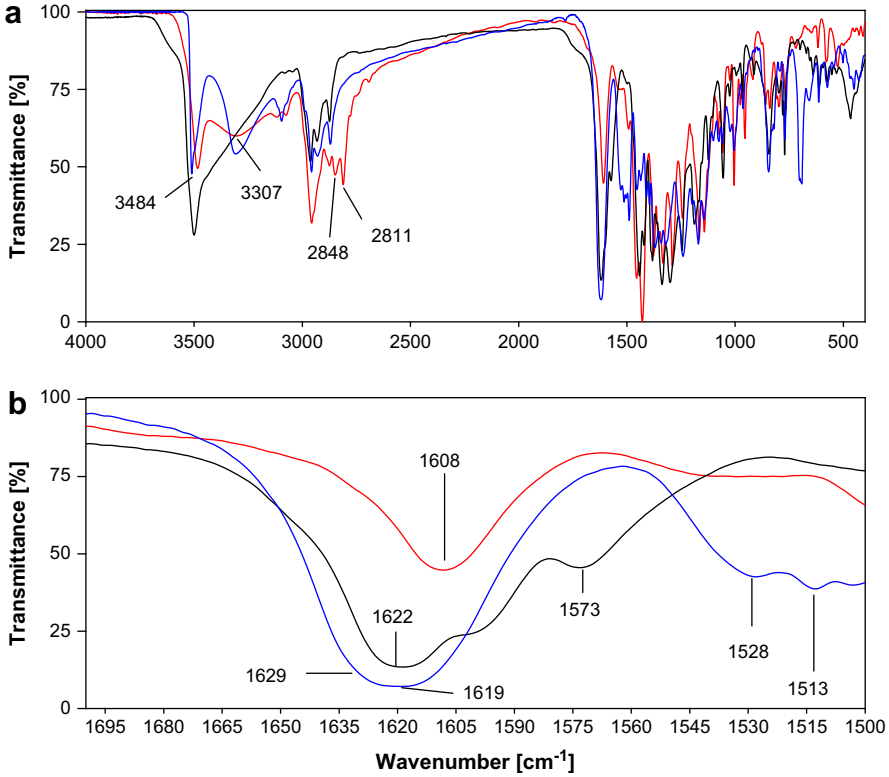

Fig. 5. The FT-IR spectra of GOS [black line], Schiff base (**7**) [blue line], hydrazone (**25**) [red line] in KBr pellet in the ranges: a) 4000–400 cm^{-1}, b) 1700–1500 cm^{-1}. (For interpretation of the references to color in this figure legend, the reader is referred to the web version of this article.)

Table 5
Selected ^{1}H and ^{13}C chemical shifts [δ, ppm] of proton and carbon atom signals of GOS and its aza-derivatives (**1**–**27**) in $CDCl_3$, CD_3CN and DMSO-d_6 solutions.

Compd.	Solvent	δ_H [ppm]						δ_C [ppm]	
		HO-1	HO-6	HO-7	H-11	HN-16	HN-17	C-7	C-11
GOS[a]	CD_3CN	5.74(s)	6.48(s)	15.24(s)	11.15(s)	–	–	151.4	201.4
				9.79(s)[c]	7.14(s)[c]				99.2[c]
				9.77(s)[c]	7.10(s)[c]				99.4[c]
1	CD_3CN	6.70(s)	7.87(bs)	–	9.72(m)	2.87(d)	–	172.5	163.4
						12.62(d)			
2	CD_3CN	6.29(s)	8.01(s)	–	9.64 (d)	13.36(bs)	–	172.6	161.6
3	CD_3CN	6.32(s)	8.01(s)	–	9.68(d)	13.36(m)	–	172.8	163.1
4	CD_3CN	6.28(s)	8.00(bs)	–	9.69(d)	13.32(q)	–	172.4	163.0
5	CD_3CN	6.28(s)	8.02(bs)	–	9.72(d)	13.35(q)	–	172.5	163.7
6	CD_3CN	6.32(s)	8.04(bs)	–	9.53(d)	13.32(m)	–	172.9	163.4
7	$CDCl_3$	5.48(s)	7.90(s)	–	9.48(d)	13.30(m)	–	172.9	162.9
8	CD_3CN	6.30(s)	8.03(bs)	–	9.62(d)	13.25(m)	–	172.3	163.1
9	$CDCl_3$	5.57(s)	7.93(s)	–	9.71(d)	13.52(dd)	–	172.7	160.7
10	CD_3CN	6.32(s)	8.05(bs)	–	9.68(d)	13.32(m)	–	172.5	162.3
11	CD_3CN	6.38(s)	8.03(bs)	–	9.67(d)	13.33(m)	–	172.6	162.7
12	DMSO-d_6	8.30(s)	9.00(bs)	–	9.79(d)	13.10(m)	–	173.2	162.1
13	DMSO-d_6	8.28(s)	9.02(bs)	–	9.76(d)	13.12(m)	–	173.0	162.3
		8.32(s)			9.79(d)			173.2	
14	CD_3CN	6.36(s)	8.06(bs)	–	9.64(d)	13.35(m)	–	172.1	162.5
		6.41(s)			9.67(d)			172.3	
15	$CDCl_3$	6.47(bs)	7.84(s)	–	10.15(d)	14.69(d)	–	173.2	152.8
		6.56(bs)			10.17(d)	14.75(d)		173.4	
16	CD_3CN	6.42(bs)	7.86(s)	–	10.06(d)	14.63(d)	–	173.0	152.9
17	CD_3CN	6.44(bs)	7.85(s)	–	10.08(d)	14.73(d)	–	173.1	152.8
18	DMSO-d_6	8.34(s)	8.98(bs)	–	9.82(d)	13.08(m)	–	173.1	162.2
19	CD_3CN	6.22(s)	7.77(s)	14.42(s)	9.57(s)	–	6.39(s)	150.3	151.4
20	CD_3CN	6.25(s)	7.78(bs)	14.46(s)	9.57(s)	–	6.39(bs)	150.2	151.7
21	CD_3CN	6.28(s)	7.75(bs)	14.49(bs)	9.59(s)	–	6.42(bs)	150.3	151.9
22	CD_3CN	6.20(s)	7.72(bs)	14.32(s)	9.55(s)	–	6.38(bs)	150.5	151.3
23[a]	DMSO-d_6	8.31(s)	8.50(bs)	14.41(s)	9.97(s)	–	12.11(s)	151.6	153.1
24[b]	DMSO-d_6	8.27(s)	8.89(bs)	14.63(s)	10.17(s)	–	12.44(s)	150.4	152.3
25	$CDCl_3$	5.73(bs)	7.01(bs)	14.62(bs)	9.55(s)	–	–	156.5	150.7
26[b]	$CDCl_3$	5.63(bs)	7.08(bs)	14.65(s)	9.64(s)	–	–	157.3	151.6
27	CD_3CN	6.49(s)	7.79(s)	12.56(bs)	9.58(s)	–	6.37(bs)	150.1	155.9

[a] Spectra from Ref. [55].
[b] Spectra from Ref. [38].
[c] Signals of diastereoisomers of the lactol–lactol form of gossypol.

In the ^{1}H NMR spectra measured in various solvents the signals of the protons of OH and those of N–H groups are separated and their chemical shifts are independent of the concentration used. This result demonstrates that all protons of these groups are involved in intramolecular hydrogen bonds and that both Schiff bases and hydrazones exist as monomers in solutions. After the addition of CD_3OD these signals vanish completely. The highest ^{1}H NMR chemical shifts are observed for the protons involved in the strongest N(16)–H···O(7) and N(16)···H–O(7) intramolecular hydrogen bonds in Schiff bases and hydrazones, respectively. A comparison of ^{1}H NMR data of gossypol aza-derivatives in $CDCl_3$, CD_3CN and DMSO-d_6 demonstrates that the positions of the O(7)–H and N(16)–H resonances seem to be dependent on the structure of the substituent at N(16) atom within gossypol aza-derivative rather than on the solvent polarity used for NMR measurements. If the gossypol aza-derivatives contain aromatic ring attached to the N(16) atom (compounds **15**–**17**), strong coupling of the π-electrons between aromatic gossypol and amine parts occurs. In this case, the strong delocalisation of the π-electrons within structures **15**–**17** is the main reason why the N(16)–H proton signals are deshielded if compared to those N(16)–H proton signals from the spectra of gossypol Schiff bases with alkyl substituents (**1**–**14**, **18**). In contrast,

Table 6
Antimicrobial activity of gossypol Schiff bases **1**, **4**, **7**, **8**, **14** and **18** as well as Gossypol (GOS); diameter of the growth inhibition zone (giz, mm) and Minimal Inhibitory Concentration (MIC, μg/ml).

Compound	**1**		**4**		**7**		**8**		**14**		**18**		GOS		CIP	
Tested strain	giz	MIC	giz	MIC	giz	MIC	giz	MIC	giz	MIC	giz	MIC	giz	MIC	giz	MIC
S. aureus NCTC 4163	15	100	14	100	18	50	16	100	15	50	–	100	16	50	26	0.5
S. aureus ATCC 25923	13	100	14	100	18	50	15	100	15	50	11	100	15	25	26	0.5
S. aureus ATCC 6538	14	100	14	100	17	50	16	100	15	50	11	100	14	25	28	0.5
S. aureus ATCC 29213	13	100	13	200	18	50	15	100	13	50	11	100	15	50	22	0.5
S. epidermidis ATCC 12228	12	100	12	100	21	25	15	100	14	50	12	100	16	25	30	0.5
B. subtilis ATCC 6633	11	50	12	50	16	25	15	50	13	25	11	100	15	12.5	40	<0.125
B. cereus ATCC 11778	11	50	12	50	15	25	15	50	14	25	11	100	15	12.5	20	0.5
E. hirae ATCC 10541	–	>400	12	>400	14	100	14	200	12	200	–	>400	14	100	–	4
M. luteus ATCC 9341	11	100	–	200	12	100	11	200	–	200	–	200	12	100	22	2
M. luteus ATCC 10240	14	50	12	100	19	50	15	100	16	50	14	100	16	25	24	1

–: denotes lack of the growth inhibition zone.
CIP – ciprofloxacin (standard antimicrobial drug, 5 μg per disc).

Table 7
Antimicrobial activity of gossypol hydrazones: **19**–**22**, **26** and Gossypol (GOS), diameter of the growth inhibition zone (giz, mm) and Minimal Inhibitory Concentration (MIC, μg/ml).

Compound	**19**		**20**		**21**		**22**		**26**		GOS		CIP	
Tested strain	giz	MIC	giz	MIC	giz	MIC	giz	MIC	giz	MIC	giz	MIC	giz	MIC
S. aureus NCTC 4163	14	100	12	200	11	200	11	400	13	50	16	50	26	0.5
S. aureus ATCC 25923	15	100	12	200	12	200	12	400	13	50	15	25	26	0.5
S. aureus ATCC 6538	13	50	12	200	11	400	11	400	12	50	14	25	28	0.5
S. aureus ATCC 29213	14	100	13	200	12	400	11	400	12	50	15	50	22	0.5
S. epidermidis ATCC 12228	15	50	12	200	14	200	13	400	14	50	16	25	30	0.5
B. subtilis ATCC 6633	13	50	11	100	11	200	12	400	12	25	15	12.5	40	<0.125
B. cereus ATCC 11778	13	50	11	100	12	200	12	400	12	25	15	12.5	20	0.5
E. hirae ATCC 10541	11	400	–	>400	–	>400	–	>400	–	200	14	100	–	4
M. luteus ATCC 9341	–	400	–	400	–	>400	–	>400	–	100	12	100	22	2
M. luteus ATCC 10240	14	50	11	100	13	100	14	400	15	25	16	25	24	1

–: denotes lack of the growth inhibition zone.
CIP – ciprofloxacin (standard antimicrobial drug, 5 μg per disc).

the chemical shifts of the O(1)–H protons depend on the kind of the solvent used. In DMSO-d_6 solution the chemical shifts of the O(1)–H signals are in the range 8.27–8.34 ppm, whereas in CD_3CN and $CDCl_3$ they are in the ranges 6.49–6.70 ppm and 5.48–6.56 ppm, respectively. It is understandable because O(1)–H protons of the aza-derivatives of gossypol in $CDCl_3$ and CD_3CN solution rather weakly interact with the π-electrons of the naphthalene rings, whereas in more polar DMSO-d_6, the O(1)–H and O(1′)–H hydroxyl groups preferentially form intermolecular hydrogen bonds with the solvent molecules.

The signal of C(11)–H proton in the ^{1}H NMR spectra of the Schiff bases appears as a doublet for compounds **2**–**18** or multiplet for compound **1** which is explained by the spin–spin coupling of C(11)–H proton with the respective ones at N(16) atom. This result indicates clearly that the Schiff bases studied occur in the enamine–enamine tautomeric form irrespectively of the kind of solvent and substituent they have. The appearance of a singlet at about 10 ppm in all spectra of gossypol hydrazones (**19**–**27**) assigned to the C(11)–H protons is the evidence of formation of a tautomeric form different than that observed for the gossypol Schiff bases, i.e. the N-imine–N-imine form. Further important information about the tautomeric forms of gossypol aza-derivatives can be obtained from the position of the C-7 carbon atom signals in the ^{13}C NMR spectra. In the spectrum of GOS the signal of C(7) carbon atom was found at 155.6 ppm in $CDCl_3$ [54] and at 151.4 ppm in CD_3CN [55], whereas the signal of C(7) carbon atom in the spectra of **19**–**27** was in the range 150.1–157.3 ppm (Table 5). The chemical shift of the C(7) signals of gossypol hydrazones (**19**–**27**), similar to those of GOS, are in the range characteristic of the C–OH carbon atoms of phenols [46,56–59]. This result shows clearly that gossypol hydrazones are present in the N-imine–N-imine tautomeric form, which is analogous to the aldehyde–aldehyde form of GOS (Scheme 1). In the corresponding spectra of gossypol Schiff bases the C(7) carbon atom resonances appear in the range 172.1–173.4 ppm, indicating the double C(7)–O bond character and the appearance of compounds **1**–**18** in the enamine–enamine tautomeric form. Similar chemical shift of the carbon atom of the carbonyl group in the aromatic system has been observed previously for the other class of compounds [59–61].

The appearance of the enamine and imine moieties within respective gossypol aza-derivatives is also reflected in the chemical shift of the O(6)–H protons in ^{1}H NMR spectra as well as by the position of C(11) resonances in the ^{13}C NMR spectra. The signals of the O(6)–H protons in the spectra of **1**–**18** are found in the ranges: 7.84–7.93 ppm in $CDCl_3$, 7.85–8.06 ppm in CD_3CN and 8.98–9.02 ppm in DMSO-d_6, whereas in the spectra of **19**–**27** in the ranges: 7.01–7.08 ppm in $CDCl_3$, 7.72–7.79 ppm in CD_3CN and 8.50–8.89 ppm in DMSO-d_6. Higher chemical shifts of O(6)–H proton

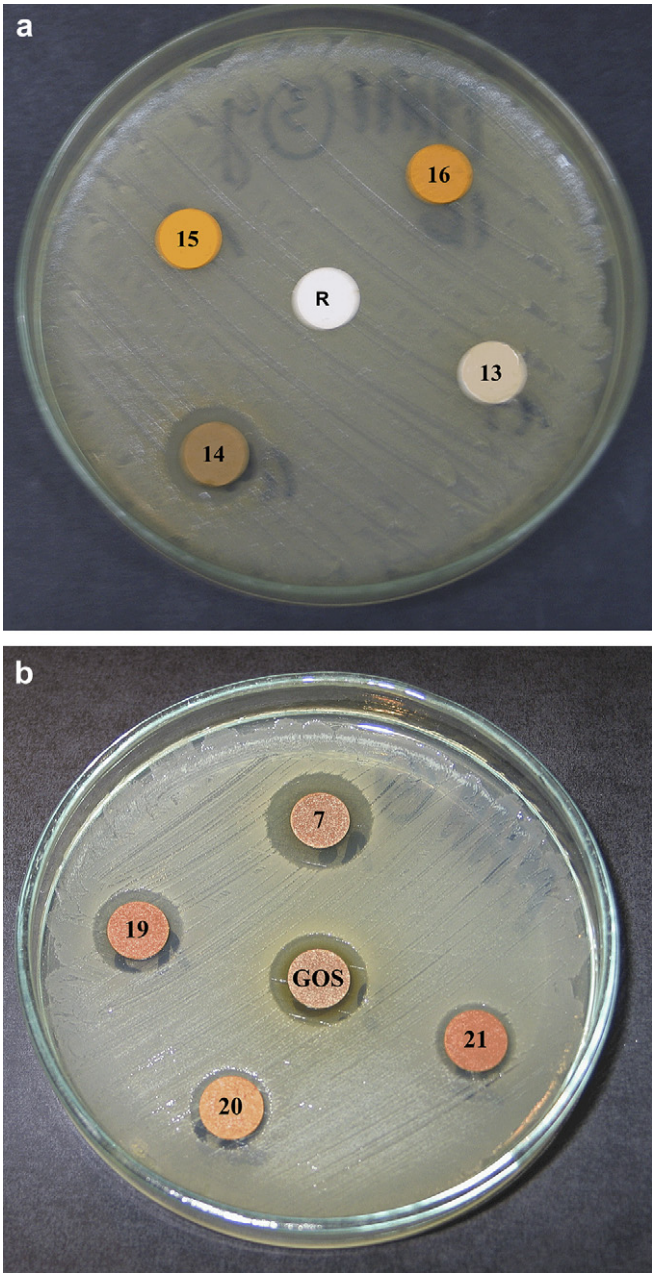

Fig. 6. Disc-diffusion method: a) the growth inhibition zone obtained on *S. aureus* ATCC 29213 for compounds **13**–**16** and DMSO [**R**]; b) the growth inhibition zone obtained on *S. aureus* ATCC 6538 for compounds **7**, **19**–**21** and GOS.

Table 8
Antimicrobial activity of gossypol and its aza-derivatives against hospital MSSA and MRSA strains of *Staphylococcus aureus*: Minimal Inhibitory Concentration (MIC, μg/ml).

Strain		**1**	**4**	**7**	**8**	**14**	**18**	**19**	**20**	**21**	**22**	**26**	GOS	CIP
206/07	MSSA	100	50	25	100	50	100	50	100	200	400	25	25	2
207/07		200	100	50	200	100	200	50	400	400	>400	50	50	0.5
208/07		100	100	50	100	100	200	50	400	400	>400	50	50	0.5
212/07		200	200	25	100	100	100	100	400	400	>400	50	50	0.5
213/07		100	100	25	100	100	100	50	200	400	400	50	50	0.5
237/07		100	100	50	100	50	100	100	200	400	400	25	25	4
238/07		100	100	50	100	50	100	50	100	400	400	25	25	0.5
239/07		100	100	50	100	100	100	100	400	400	400	25	25	0.5
242/07		50	50	12.5	50	25	100	50	50	100	200	12.5	12.5	0.5
243/07		100	100	50	100	100	200	100	400	400	>400	25	25	0.5
136/06	MRSA	100	50	50	100	25	100	100	100	200	400	50	50	>8
140/06		100	100	50	100	100	100	50	200	200	400	50	50	>8
141/06		100	200	50	100	100	100	100	200	400	400	50	50	>8
143/06		100	100	50	100	100	100	50	400	400	>400	50	50	>8
144/06		100	200	50	200	100	100	100	200	400	400	50	50	>8
146/06		100	100	50	100	50	100	100	200	200	400	50	50	>8
200/07		100	100	50	100	100	200	50	200	400	>400	50	50	> 8
217/07		200	200	100	200	100	200	100	400	200	>400	50	50	>8
218/07		100	100	50	100	100	100	100	200	400	>400	50	50	4
236/07		100	50	50	100	50	100	100	100	100	400	25	50	1

CIP – ciprofloxacin (standard antimicrobial drug).

signals in the spectra of **1**–**18** in comparison to those of **19**–**27** demonstrate that in the former the hydroxyl groups are involved in stronger intramolecular hydrogen bonds than in the latter ones. This fact can be explained by the presence of the C(7)═O carbonyl group and C(7)–OH hydroxyl group in the naphthalene ring of Schiff bases **1**–**18** and hydrazones **19**–**27**, respectively. The C(11) carbon atom is connected by the N(16)═(C11) double bond in the imine and C(11)═C(8) double bond in the enamine moieties. The ^{13}C NMR spectra show the C(11) carbon atom signals in ranges: 160.7–163.7 ppm for 1–18 /except of 15–17/ and 150.7–155.9 ppm for **19**–**27**. These different chemical shift ranges noted for the Schiff bases and hydrazones containing at N(16) and N(17) atoms alkyl substituents can be a result of different electron density distribution within two different enamine and imine moieties. However, the C(11) carbon atom signals in the spectra of **15**–**17** Schiff bases containing aromatic substituents are at 152.8 and 152.9 ppm, in the range characteristic of **19**–**27** gossypol hydrazones. The explanation of this fact is the strong π-electron coupling between the amine and gossypol parts in the gossypol Schiff bases with aniline derivatives.

3. Antimicrobial activity

Gossypol and a series of its derivatives (Schiff bases and hydrazones) were tested in vitro for antibacterial and antifungal activity. The results collected in Tables 6 and 7 demonstrate that gossypol and its 11 aza-derivatives are active against Gram-positive bacteria. Good activity was observed for GOS (MICs values of standard strains were 12.5–100 μg/ml) and derivatives **7**, **14**, **19** and **26** (MICs 25–200 μg/ml). Compounds **1**, **4**, **8**, **18** and **20** showed moderate activity (MICs values between 100 and 200 μg/ml). Derivatives **21** and **22** exhibit low antibacterial activity (MICs 200 to >400 μg/ml). The antimicrobial test results on *Staphylococcus aureus* ATCC 29213 and ATCC 6538, shown in Fig. 6a and b, prove that compounds **7**, **14** and **19** have activity comparable with that of GOS. A comparison of the antimicrobial activity of gossypol hydrazones (**19**–**22**) and gossypol Schiff bases (**3**–**5**) containing oxaalkyl chains has shown that generally the former are more active against strains tested than the latter ones. This result can be also related with the presence of different tautomeric forms within gossypol hydrazones and Schiff bases because the length of the oxaalkyl chains in both types of compounds is comparable. Generally, for the active hydrazones **19**–**21** their antibacterial activity is correlated with the oxaalkyl chain length, i.e. the longer the oxaalkyl chain the lower the antibacterial activity (Scheme 2, Table 7). The only one active gossypol Schiff base among those containing oxaalkyl chains is compound **4**. The activity of compound **4** can be probably a result of the presence in its structure of non-polar terminal n-butyl groups, which probably enable better interaction of this derivative with the lipid bilayers of bacteria. The relatively higher antibacterial activity of derivative **7** can be a result of the presence in its structure of a thiophene alkyl derivative. It is well known that many alkyl derivatives of thiophene have great antibacterial activity i.e. are inhibitors of bacterial fatty acid synthetase (Type II) [62,63]. The results of the biological activity tests indicate also that Schiff bases containing heterocyclic aromatic rings in their structures like thiophene (**7**), indol (**8**), imidazol (**14**) have greater antibacterial activity than those containing aliphatic heterocyclic systems (**6**, **9**, **10**, **11**, **17**). The exception is compound **18**, whose antibacterial activity can be related to the enhanced ability of Na^+ or K^+ cation complexation in comparison to the other ones [35,64]. It is interesting to note that for hydrazone **24** containing a heterocyclic aromatic ring – thiophene, no activity was noted against bacteria, whereas the activity of hydrazone **26**, containing aliphatic piperazine ring, was significant.

The modification of the gossypol molecule by the amines containing boron or silicon atoms in their structures give compounds (**12**, **16**) inactive against microorganisms tested. All compounds examined were inactive against Gram-negative rods and yeast-like organisms.

S. aureus is one of the most significant human pathogens responsible for nosocomial infections. Methicillin-resistant strains (MRSA) are resistant to all beta-lactams and they are often resistant to some other widely used antibiotics. It is well known that defence mechanism of *S. aureus* against simple naphthalene derivatives containing carbonyl groups is based on the enzymatic reduction process of C═C bonds [65]. Despite this fact the preliminary test by disc-diffusion method show the activity of GOS and **11**, its aza-derivatives containing naphthalene moieties, against standard *S. aureus* strains. The next step of biological tests was the evaluation of active compounds GOS, **1**, **4**, **7**, **8**, **14**, **18**–**22**, **26** for clinical isolates of methicillin-susceptible (10 strains MSSA) and methicillin-resistant (10 strains MRSA). According to Table 8 results, the compounds tested show a broad spectrum of activity with MIC values 12.5–400 (and higher) μg/ml. The best activity against both MSSA and MRSA strains of *S. aureus* (MICs values 12.5–50 μg/ml), among gossypol aza-derivatives studied, shows derivative **26**. It is interesting to

note that only one from among MSSA and MRSA strains tested, is the least resistant to all compounds (242/07 strain, MICs = 12.5–200 μg/ml).

4. Conclusion

Gossypol Schiff bases **1**–**18** and gossypol hydrazones **19**–**27** have been synthesized and tested for antimicrobial activity. For the first time the crystal structure of gossypol hydrazone (**25**) has been determined and compared to the respective one of gossypol Schiff base (**7**). The structures of **7** and **25**, determined by the X-ray method, reveal the presence of two different tautomeric forms of gossypol aza-derivatives i.e. for gossypol Schiff base (**7**) the enamine–enamine and for gossypol hydrazone (**25**) the imine–imine form. The structural parameters of **7** and **25** in the solid state indicate that the structures of both tautomers are strongly stabilized by the intra- and intermolecular hydrogen bonds assisted by the resonance of the π-electrons in the aromatic system. The FT-IR spectra of the crystals of **7** and **25** indicate the presence of two different tautomers of the aza-derivatives in solid, which is in agreement with the X-ray results. NMR studies of **1**–**27** gossypol derivatives have proved that in solutions, the respective tautomeric forms are conserved. Analysis of the ^{1}H and ^{13}C NMR chemical shifts of the two series of gossypol aza-derivatives indicated the ^{1}H and ^{13}C chemical shift ranges, characteristic of the enamine–enamine and imine–imine tautomers, which can be used for qualitative distinction between them. In less polar solvent such as $CDCl_3$, the tautomeric forms of gossypol derivatives are mainly stabilized by the intramolecular hydrogen bonds, whereas in more polar ones, such as DMSO-d_6, by the inter- and intramolecular hydrogen bonds. GOS and its derivatives **1**–**27** were tested for their antimicrobial activities against Gram-positive bacteria, Gram-negative bacteria and yeast-like organisms. Preliminary test by disc-diffusion method evidenced the activity of GOS and **11**, its aza-derivatives against standard *S. aureus* strains and therefore, they were further evaluated for activity against clinical isolates of methicillin-susceptible (10 strains MSSA) and methicillin-resistant strains (10 strains MRSA). It is interesting to note that compounds **7**, **14** and **26** proved to be even more active than gossypol against some MSSA and MRSA strains. If we take into account the results of biological tests on two series MSSA and MRSA strains, compound **26** reveals the activity comparable and in one case higher than that of GOS. The antimicrobial tests of various gossypol aza-derivatives suggested that especially heterocyclic derivatives of gossypol should be considered as candidates for new and effective antibacterial agents based on gossypol.

5. Experimental

5.1. General

DMSO-d_6, $CDCl_3$ and $CHCl_3$ for spectroscopic measurements as well as ammonia, allylamine, (*R*)-tetrahydrofurfurylamine, 2-thiopheneethyl-amine, 5-methoxytryptamine, ethyl 4-amino-1-piperidine carboxylate, 3-morpholinopropylamine, 1-(3-aminopropyl)-2-pyrrolidinone, (3-aminopropyl)-trimethoxysilane, L-arginine methyl ester, L-carnosine, *N*-(4-Aminobenzoyl)-L-glutamic acid diethyl ester, 4-(4,4,5,5–tetramethyl-1,3,2-dioxaborolan-2-yl)-aniline, 4′-aminobenzo-15-crown-5, 2-(aminomethyl)-18-crown-6, hydrazine, ethyl 3-hydrazino-3-oxopropionate, *N*-amino-*N*′-hydroxyethylpiperazine used for synthesis of gossypol derivatives were purchased from Aldrich. GOS was extracted from cotton seeds of *Gossypium herbaceum* following the procedure given in Ref. [66]. 5-Hydroxy-3-oxa-pentylamine; 3,6-dioxa-decylamine; 3,6,9-trioxa-decylamine were synthesized following our procedure given in Ref. [14]. Schiff bases of gossypol **1**–**6**, **8**, **10**, **11**, **13**, **14**, **16**–**18** were synthesized following our procedures given in Refs. [31–35,38,43,67,68], whereas hydrazones of gossypol **19**–**24**, **26**, **27** – following our procedures given in Refs. [19,38,69,70].

For **7** and **25** monocrystals suitable to X-ray study were obtained. The samples selected for the single-crystal X-ray diffraction measurement were dark-brown (**7**) and brightly yellow (**25**) parallelepipeds without well-developed faces. They were stable under normal conditions and X-ray diffraction data were measured on a Kuma KM-4 CCD diffractometer at room temperature. Their structures were solved by direct methods [71] and refined by full-matrix least-squares [72]. Five H-atoms at N(16) and N(16′) in **7** molecule and at O(2), O(3) and O(1′) in **25** molecule were found in difference Fourier maps and all other H-atoms were located from the molecular geometry (C–H 0.93–0.98 and C–O 0.82–0.85 Å) and their U_{iso}s were related to the thermal vibrations of their carriers. The details of the measurements, crystals data, structures' solution and refinement are given in Table 1. The crystallographic-information-files (CIF) have been deposited with the Cambridge Crystallographic Database Center as a supplementary publication: for (**7**) No. CCDC 705280 and for (**25**) No. CCDC 705281.

The ^{1}H and ^{13}C measurements were performed in $CDCl_3$, CD_3CN and DMSO-d_6 using Bruker Avance 600 MHz spectrometer. The operating frequency for ^{1}H measurements was 600.08 MHz; pulse width corresponding to the flip angle of 45°; spectral width, swh = 9842.5 Hz; acquisition time at = 0.2 s; relaxation delay d_1 = 1.0 s; T = 293.0 K, TMS as the internal standard was used. No window function or zero filling were used. Digital resolution was 0.2 Hz/point. ^{13}C NMR spectra were recorded at the operating frequency 150.454 MHz; pulse width corresponding to the flip angle of 60°; sw = 19,000 Hz; at = 1.8 s; d_1 = 1.0 s; T = 293.0 K and TMS as the internal standard. Line broadening parameters of 0.5 or 1 Hz were applied. ^{1}H and ^{13}C resonances were unambiguously assigned on the basis of the HMBC, HSQC, COSY and NOESY correlation spectra.

The FT-IR spectra of gossypol and its aza-derivatives were recorded in the KBr pellet (1.5 mg/200 mg). The FT-IR spectra were taken with an IFS 113v FT-IR spectrophotometer (Bruker, Karlsruhe) equipped with a DTGS detector; resolution 2 cm^{-1}, NSS = 125, range 4000–400 cm^{-1}. The Happ–Genzel apodization function was used. All manipulations with the substances were performed in a carefully dried and CO_2-free glove box.

The ESI (Electrospray Ionisation) mass spectra were recorded on a Waters/Micromass (Manchester, UK) ZQ mass spectrometer equipped with a Harvard Apparatus syringe pump. All samples of aza-derivatives of gossypol and gossypol were prepared in acetonitrile. The measurements were performed for the solutions of each gossypol aza-derivative (1×10^{-5} mol dm^{-3}) mixed with HCOOH (1×10^{-5} mol dm^{-3}). The samples were infused into the ESI source using a Harvard pump at a flow rate of 20 μl min^{-1}. The ESI source potentials were: capillary 3 kV, lens 0.5 kV, extractor 4 V. The standard ESI mass spectra were recorded at 30 V. The source temperature was 120 °C and the dessolvation temperature was 300 °C. Nitrogen was used as the nebulizing and dessolvation gas at flow-rates of 100 and 300 dm^3 h^{-1}, respectively. Mass spectra were acquired in the positive ion detection mode with unit mass resolution at a step of 1 m/z unit. The mass range for ESI experiments was from m/z = 100 to m/z = 2000.

The elemental analysis of new gossypol aza-derivatives was carried out on Vario ELIII (Elementar, Germany).

5.2. General procedure for the preparation of a new Schiff bases and hydrazones of gossypol (*7*, *9*, *12*, *15*, *25*)

Aza-derivatives of gossypol were synthesized by addition of 2.00 mmol of the respective amine or hydrazine dissolved in 50 mL

of absolute ethanol to a 1 mmol of gossypol solution in 180 mL of absolute ethanol. The mixture was stirred under reflux for 3 h under argon atmosphere. The progress of the reaction was monitored by the ESI$^+$ MS spectra (decreasing intensity of the peak $m/z = 519$ $[GOS + H]^+$). After cooling of the mixture, the products precipitated and were filtered off and dried under reduced pressure. Crude precipitates were recrystallised from 1:1 CH_2Cl_2/MeOH (**7**, **25**), EtOH (**12**, **15**) or CH_3CN (**9**) solutions. Hydrazones and Schiff bases of gossypol were obtained as yellow, orange or orange-brown solids.

^{1}H NMR of (**7**) (600 MHz, $CDCl_3$), δ_H values in ppm: HO-1 (2H, 5.48, s); H-4 (2H, 7.50, s); HO-6 (2H, 7.90, s); H-11 (2H, 9.48, d, $^3J_{H16–H11} = 9.8$ Hz); H-12 (6H, 2.02, s); H-13 (2H, 3.65, sept, $^3J_{H13–H14,15} = 6.8$ Hz); H-14 and H-15 (12H, 1.45 and 1.44, d, $^3J = 6.8$ Hz); HN-16 (2H, 13.30, m); H-17 (4H, ~3.65, m); H-18 (4H, 3.13, t, $^3J_{H18–H17} = 6.9$ Hz); H-20 (2H, 6.77, d, $^3J_{H20–H21} = 3.4$ Hz); H-21 (2H, 6.83, t, $^3J_{H21–H22} = 4.9$ Hz and $^3J_{H21–H20} = 3.4$ Hz); H-22 (2H, 7.05, d, $^3J_{H21–H22} = 4.9$ Hz). ^{13}C NMR of (**7**) (150 MHz, $CDCl_3$), δ_C values in ppm: C-1 (148.9); C-2 (115.8); C-3 (131.8); C-4 (118.2); C-5 (127.4); C-6 (147.1); C-7 (172.9); C-8 (103.3); C-9 (114.6); C-10 (129.0); C-11 (162.9); C-12 (20.0); C-13 (27.4); C-14 and C-15 (20.4 and 20.5); C-17 (52.2), C-18 (31.3); C-19 (139.3); C-20 (126.0); C-21 (127.2); C-22 (124.4). ESI$^+$ MS $m/z = 737$ $[M + H]^+$, m.p. = 198–202 °C, Elemental Analysis Calcd.: C = 68.45%, H = 6.02%, N = 3.80%; Found: C = 68.42%, H = 6.00%, N = 3.81%.

^{1}H NMR of (**9**) (600 MHz, $CDCl_3$), δ_H values in ppm: HO-1 (2H, 5.57, s); H-4 (2H, 7.59, s); HO-6 (2H, 7.93, s); H-11 (2H, 9.71, d, $^3J_{H11–H16} = 12.0$ Hz); H-12 (6H, 2.11, s); H-13 (2H, 3.72, sept, $^3J_{H13–H14,15} = 7.0$ Hz); H-14 and H-15 (12H, 1.53 and 1.52, d, $^3J_{H13–H14,15} = 7.0$ Hz); HN-16 (2H, 13.52, dd, $^3J_{H16–H11} = 12.0$ Hz and $^3J_{H16–H17} = 7.1$ Hz); H-17 (2H, ~4.10, m); H-18$_{axial}$ and H-18a$_{axial}$ (2H, 1.74, m); H-18$_{equatorial}$ and H-18a $_{equatorial}$ (2H, 2.04, m); H-19 $_{equatorial}$ (1H, ~4.10, m); H-19a $_{equatorial}$ (1H, 3.56, m); H-19 $_{axial}$ and H-19a $_{axial}$ (2H, 3.03, m); H-22 (4H, 4.13, q, $^3J_{H22–H23} = 7.1$ Hz); H-23 (6H, 1.25, t, $^3J_{H22–H23} = 7.1$ Hz). ^{13}C NMR of (**9**) (150 MHz, $CDCl_3$), δ_C values in ppm: C-1 (148.8); C-2 (115.7); C-3 (131.9); C-4 (118.3); C-5 (127.6); C-6 (147.1); C-7 (172.7); C-8 (103.3); C-9 (114.5); C-10 (129.0); C-11 (160.7); C-12 (20.1); C-13 (27.4); C-14 and C-15 (20.3); C-17 (56.9); C-18 (32.5); C-19 (42.0); C-21 (155.3); C-22 (61.6); C-23 (14.7). ESI$^+$ MS $m/z = 827$ $[M + H]^+$, m.p. = 179–184 °C, Elemental Analysis Calcd.: C = 66.81%, H = 7.07%, N = 6.77%; Found: C = 66.82%, H = 7.04%, N = 6.75%.

^{1}H NMR of (**12**) (600 MHz, DMSO-d_6), δ_H values in ppm: HO-1 (2H, ~8.3, bs); H-4 (2H, 7.42, s); HO-6 (2H, ~9.00, bs); H-11 (2H, 9.79, d, $^3J_{H11–H16} = 13.6$ Hz); H-12 (6H, 1.94, s); H-13 (2H, 3.70, sept, $^3J_{H13–H14,15} = 6.9$ Hz); H-14 and H-15 (12H, 1.43 and 1.41, d, $^3J_{H13–H14,15} = 6.9$ Hz); HN-16 (2H, 13.10, m, $^3J_{H11–H16} = 13.6$ Hz and $^3J_{H16–H17} = 7.2$ Hz); H-17 (4H, 2.93, dt, $^3J_{H17–H16} = 13.6$ Hz and $^3J_{H17–H18} = 6.8$ Hz); H-18 (4H, 1.69, m, $^3J_{H17–H18} = 6.8$ Hz and $^3J_{H18–H19} = 7.1$ Hz); H-19 (4H, 0.72, t, $^3J_{H18–H19} = 7.1$ Hz); H-20-22 (18H, 4.42, s). ^{13}C NMR of (**12**) (150 MHz, DMSO-d_6), δ_C values in ppm: C-1 (150.2), C-2 (120.6); C-3 (131.4); C-4 (116.9); C-5 (126.7); C-6 (146.9); C-7 (173.2); C-8 (103.7); C-9 (115.9); C-10 (128.1); C-11 (162.1); C-12 (20.5); C-13 (26.8); C-14 and C-15 (20.8); C-17 (47.2); C-18 (28.6); C-19 (12.8); C-20-22 (42.1). ESI$^+$ MS $m/z = 841$ $[M + H]^+$, m.p. = 149–153 °C, Elemental Analysis Calcd.: C = 59.98%, H = 7.19%, N = 3.33%; Found: C = 59.96%, H = 7.18%, N = 3.30%.

^{1}H NMR of (**15**) (600 MHz, $CDCl_3$), δ_H values in ppm: HO-1 (2H, 6.47, bs and 6.56, bs); H-4 (2H, 7.56, s and 7.60, s); HO-6 (2H, 7.84, s); H-11 (2H, 10.15, d and 10.17, d, $^3J_{H11–H16} = 8.5$ Hz, $^3J_{H11–H16} = 7.7$ Hz); H-12 (6H, 2.18, s); H-13 (2H, 3.68, sept, $^3J_{H13–H14,15} = 5.9$ Hz); H-14 and H-15 (12H, 1.54, d, $^3J_{H13–H14,15} = 5.9$ Hz); HN-17 (2H, 14.69, d and 14.75, d, $^3J_{H11–H16} = 8.5$ Hz, $^3J_{H11–H16} = 7.7$ Hz); H-18 and H-19 (4H, 7.27 dd and 7.29 dd, $^3J_{H21–H22} = 8.0$ Hz and $^4J_{H18–H19} = 2.5$ Hz); H-20 and H-21 (4H, 7.73 dd and 7.76 dd, $^3J_{H18–H20} = 8.0$ Hz and $^4J_{H18–H19} = 2.5$ Hz); HN-24 (2H, 7.09, d and 7.16, d , $^3J_{H24–H25} = 7.1$ Hz); H-25 (2H, 4.69, m, $^3J_{H24–H25} = 7.1$ Hz, $^3J_{H25–H29} = 4.4$ Hz); H-27 (4H, 4.24, m, $^3J_{H27–H28} = 7.2$ Hz); H-28 (6H, 1.32, m, $^3J_{H27–H28} = 7.2$ Hz); H-29 (4H, ~2.2, m, $^3J_{H25–H29} = 4.4$ Hz, $^3J_{H29–H30} = 7.9$ Hz); H-30 (4H, ~2.5, m, $^3J_{H30–H29} = 7.9$ Hz); H-32 (4H, 4.08, m, $^3J_{H32–H33} = 7.1$ Hz); H-33 (6H, 1.21, m, $^3J_{H32–H33} = 7.1$ Hz). ^{13}C NMR of (**15**) (150 MHz, $CDCl_3$), δ_C values in ppm: C-1 (149.9), C-2 (117.2*); C-3 (130.0 and 130.2); C-4 (118.6); C-5 (128.5); C-6 (146.7); C-7 (173.2 and 173.4); C-8 (106.0); C-9 (114.4); C-10 (129.7); C-11 (152.7); C-12 (20.2); C-13 (27.6); C-14 and C-15 (20.3); C-17 (133.6); C-18 and C-19 (117.4*); C-20 and C-21 (128.9); C-22 (142.2); C-23 (165.8 and 166.0); C-25 (52.5); C-26 (175.3); C-27 (61.8); C-28 (14.2**); C-29 (27.1); C-30 (30.5); C-31 (171.9); C-32 (60.9); C-33 (14.1**); *,** – overlapped signals. ESI$^+$ MS $m/z = 1127$ $[M + H]^+$, m.p. = 214–216 °C, Elemental Analysis Calcd.: C = 66.06%, H = 6.26%, N = 4.97%; Found: C = 66.04%, H = 6.25%, N = 4.93%.

^{1}H NMR of (**25**) (600 MHz, $CDCl_3$), δ_H values in ppm: HO-1 (2H, 5.73, bs); H-4 (2H, 7.59, s); HO-6 (2H, 7.01, bs); HO-7 (2H, 14.62, bs); H-11 (2H, 9.55, s); H-12 (6H, 2.03, s); H-13 (2H, 3.76, sept, $^3J_{H13–H14,15} = 7.0$ Hz); H-14 and H-15 (12H, 1.45 and 1.47, d, $^3J_{H13–H14,15} = 7.0$ Hz); H-18 and H18a (8H, 3.02, m); H-19 and H19a (8H, 2.43, m); H-21 (6H, 2.20, s). ^{13}C NMR of (**25**) (150 MHz, $CDCl_3$), δ_C values in ppm: C-1 (148.9), C-2 (116.0); C-3 (131.3); C-4 (117.7); C-5 (126.6); C-6 (141.6); C-7 (156.5); C-8 (105.9); C-9 (114.6); C-10 (129.6); C-11 (150.7); C-12 (20.2); C-13 (27.3); C-14 and C-15 (20.4); C-18 and C18a (53.1); C-19 and C-19a (54.0); C-21 (45.6). ESI$^+$ MS $m/z = 713$ $[M + H]^+$, m.p. = 163–166 °C, Elemental Analysis Calcd.: C = 67.39%, H = 7.35%, N = 11.79%; Found: C = 67.37%, H = 7.32%, N = 11.73%.

5.3. Antimicrobial tests

Microorganisms used in this study were as follows: Gram-positive bacteria: *S. aureus* NCTC 4163, *S. aureus* ATCC 25923, *S. aureus* ATCC 6538, *S. aureus* ATCC 29213, *S. epidermidis* ATCC 12228, *Bacillus subtilis* ATCC 6633, *Bacillus cereus* ATCC 11778, *Enterococcus hirae* ATCC 10541, *Micrococcus luteus* ATCC 9341, *M. luteus* ATCC 10240 as well as various clinical isolates of *S. aureus* (MSSA and MRSA strains), Gram-negative rods: *Escherichia coli* ATCC 10538, *E. coli* ATCC 25922, *E. coli* NCTC 8196, *Proteus vulgaris* NCTC 4635, *Pseudomonas aeruginosa* ATCC 15442, *P. aeruginosa* NCTC 6749, *P. aeruginosa* ATCC 27853, *Bordetella bronchiseptica* ATCC 4617 and yeast-like organisms: *Candida albicans* ATCC 10231, *C. albicans* ATCC 90028, *Candida parapsilosis* ATCC 22019.

Antimicrobial activity was examined by the disc-diffusion and MIC method under standard conditions using Mueller–Hinton II agar medium (Becton Dickinson) for bacteria and RPMI agar with 2% glucose (Sigma) for yeasts, according to CLSI (previously NCCLS) guidelines. The compounds giving some growth inhibition zone in disc-diffusion assay were tested by the twofold serial agar dilution technique to determine their minimal inhibitory concentration (MIC) values. For the disc-diffusion method, sterile filter paper discs (9 mm diameter, Whatman No 3 chromatography paper) were dripped with the compound solutions tested (in DMSO) to load 400 μg of a given compound per disc. Dry discs were placed on the surface of an appropriate agar medium. The results (diameter of the growth inhibition zone) were read after 18 h (for bacteria) or 24 h (for yeasts) of incubation at 35 °C. For MICs determination, gossypol and its aza-derivatives were dissolved in DMSO. Concentrations of the agents tested in solid medium ranged from 3.125 to 400 μg/ml. The final inoculum of all microorganisms studied was 10^4 CFU mL^{-1} (colony forming units per ml), except the final inoculums for *E. hirae* ATCC 10541, which was 10^5 CFU mL^{-1}. A control test was also performed containing inoculated broth supplemented with DMSO which was found inactive against tested

strains. Minimal inhibitory concentrations were read after 18 h of incubation at 35 °C. Ciprofloxacin was used as a standard antibacterial drug. The results are summarized in Tables 6–8. Hospital strains of *S. aureus* were isolated from different biological materials of patients hospitalized in one of the Warsaw hospitals. All microorganisms used were obtained from the collection of the Department of Pharmaceutical Microbiology, Medical University of Warsaw, Poland.

Clinical and Laboratory Standards Institute, Performance Standards for Antimicrobial Disc Susceptibility Tests; Approved Standard M2-A9. Clinical and Laboratory Standards Institute, Wayne, PA, USA, 2006; Clinical and Laboratory Standards Institute, Methods for Dilution Antimicrobial Susceptibility Tests for Bacteria That Grow Aerobically; Approved Standard M7-A7. Clinical and Laboratory Standards Institute, Wayne, PA. USA, 2006.

Acknowledgements

Financial assistance of the Polish Ministry of Science and Higher Education – Grant No. N204 056 32/1432 is gratefully acknowledged by P. Przybylski.

References

[1] C.R. Benedict, G.S. Martin, J. Liu, L. Puckhaber, C.W. Magill, Phytochemistry 65 (2004) 1351–1359.
[2] K. Dodou, Exp. Opin. Invest. New Drug 14 (2005) 1419–1434.
[3] T.-S. Lin, R.F. Schinazi, J. Zhu, E. Birks, R. Carbone, Y. Si, K. Wu, L. Huang, W.H. Prusoff, Biochem. Pharmacol. 46 (1993) 251–255.
[4] R.E. Royer, L.M. Deck, T.J. Vander Jagt, F.J. Martinez, R.G. Mills, S.A. Young, D.L. Vander Jagt, J. Med. Chem. 38 (1995) 2427–2432.
[5] L.B. Pacheco, J. Castro-Garza, E. Perez-Eguia, H. Zepeda-Herrera, K. Chico-Mijares, M.P. Carranza-Rosales, S. Said-Fernandez, M.T. Gonzalez-Garza, Pharm. Sci. 2 (1996) 333–334.
[6] T.S. Lin, R. Schinazi, B.P. Griffith, E.M. August, B.F.H. Eriksson, D.-K. Zgeng, L. Huang, W.H. Prusoff, Antimicrob. Agents Chem. 33 (1989) 2149–2151.
[7] Y.-F. Hu, C.-J.G. Chang, R.W. Brueggemeier, Y.C. Lin, Cancer Lett. 87 (1994) 17–23.
[8] T. Coyle, S. Levante, M. Shetler, J. Winfield, J. Neuro-oncol. 19 (1994) 25–35.
[9] W. Ye, H.-L. Chang, L.-S. Wang, Y.-W. Huang, S. Shu, M.K. Dowd, P.J. Wan, Y. Sugimoto, Y.C. Lin, Anticancer Res. 27 (2007) 107–116.
[10] M.E. Mace, R.D. Stipanovic, A.A. Bell, Nat. Toxins 1 (1993) 294–295.
[11] K.J. Abraham, M.L. Pierce, M. Essenberg, Phytochemistry 52 (1999) 829–836.
[12] P. Kovaci, Curr. Med. Chem. 10 (2003) 2711–2718.
[13] J.A. Kenar, J. Am. Oil Chem. Soc. 83 (2006) 269–302.
[14] P. Przybylski, B. Brzezinski, Biopolymers (Biospectroscopy) 67 (2002) 61–69.
[15] V.-T. Dao, M.K. Dowd, C. Gaspard, M.-T. Martin, J. Hećmez, O. Laprećvote, M. Mayer, R.J. Michelot, Bioorg. Med. Chem. 11 (2003) 2001–2006.
[16] K.Zh. Rezhepov, Kh.L. Ziyaev, N.I. Baram, F.G. Kamaev, M.G. Levkovich, A.M. Saiitkulov, A.I. Ismailov, Chem. Nat. Compd. 39 (2003) 358–361.
[17] V.-T. Dao, M.K. Dowd, M.-T. Martin, C. Gaspard, M. Mayer, R.J. Michelot, Eur. J. Med. Chem. 39 (2004) 619–624.
[18] T.T. Quang, K.P.P. Nguyen, P.E. Hansen, Magn. Res. Chem. 43 (2005) 302–308.
[19] P. Przybylski, W. Schilf, W. Lewandowska, B. Brzezinski, Biopolymers 83 (2006) 213–225.
[20] K. Dodou, R.J. Anderson, W.J. Lough, D.A.P. Small, M.D. Shelley, P.W. Groundwater, Bioorg. Med. Chem. 13 (2005) 4228–4237.
[21] V. Razakantoanina, N.K.P. Phung, G. Jaureguiberry, Parasitol. Res. 86 (2000) 665–668.
[22] X.S. Liang, A.J. Rogers, C.L. Webber, T.J. Ormsby, M.E. Tiritan, S.A. Matlin, C.C. Benz, Invest. New Drug 13 (1995) 181–186.
[23] M.D. Shelley, L. Hartley, P.W. Groundwater, R.G. Fish, Anti-cancer Drugs 11 (2000) 209–216.
[24] K.Zh. Rezhepov, Kh.L. Ziyaev, N.I. Baram, A.I. Ismailov, F.G. Kamaev, A.M. Saiitkulov, Chem. Nat. Compd. 38 (2002) 319–322.
[25] R.E. Royer, R.G. Mills, S.A. Young, D.L. Vander Jagt, Pharmacol. Res. 31 (1995) 49–52.
[26] M. Yildirim-Aksoy, C. Lim, M.K. Dowd, P.J. Wan, P.H. Klesius, C. Shoemaker, J. Appl. Microbiol. 97 (2004) 87–92.
[27] G. Tegos, F.R. Stermitz, O. Lomovskaya, K. Lewis, Antimicrob. Agents Chem. 46 (2002) 3133–3141.
[28] S. Boonsri, Ch. Karalai, Ch. Ponglimanot, S. Chantrapromma, A. Kanjana-Opas, J. Nat. Prod. 71 (2008) 1173–1177.
[29] M. Essenberg, M.d'A. Doherty, B.K. Hamilton, B.T. Henning, E.C. Cover, S.J. McFaul, W.M. Johnson, Phytopathology 72 (1982) 1349–1356.
[30] M. Essenberg, M.L. Pierce, B. Hamilton, E.C. Cover, V.E. Scholes, P.E. Richardson, Physiol. Mol. Plant Pathol. 41 (1992) 85–99.
[31] P. Przybylski, K. Pyta, M. Ratajczak-Sitarz, A. Katrusiak, B. Brzezinski, Struct. Chem. 19 (2008) 983–995.
[32] P. Przybylski, F. Bartl, B. Brzezinski, Biopolymers 65 (2002) 111–120.
[33] P. Przybylski, G. Bejcar, A. Huczyński, G. Schroeder, B. Brzezinski, F. Bartl, Biopolymers 82 (2006) 521–535.
[34] P. Przybylski, G. Schroeder, B. Brzezinski, Phys. Chem. Chem. Phys. 4 (2002) 6137–6143.
[35] P. Przybylski, G. Schroeder, B. Brzezinski, J. Mol. Struct. 699 (2004) 65–77.
[36] V.-T. Dao, C. Gaspard, M. Mayer, G.H. Werner, S.N. Nguyen, R.J. Michelot, Eur. J. Med. Chem. 35 (2000) 805–813.
[37] S.A. Matlin, S. Roshdy, Q.B. Cass, L.C.G. Freitas, R.L. Longo, I. Malvestiti, J. Braz. Chem. Soc. 1 (1990) 128–135.
[38] P. Przybylski, W. Schilf, B. Kamieński, B. Brzezinski, F. Bartl, Magn. Res. Chem. 46 (2008) 534–544.
[39] K.M. Beketov, S.A. Talipov, B.T. Ibragimov, K.D. Praliev, T.F. Aripov, Kristallografiya (Russ.) 48 (2003) 691–694.
[40] P. Przybylski, M. Ratajczak-Sitarz, A. Katrusiak, G. Wojciechowski, W. Schilf, B. Brzezinski, J. Mol. Struct. 655 (2003) 293–300.
[41] M. Gdaniec, J. Incl. Phenom. Macrocycl. Chem. 17 (1994) 365–376.
[42] S.A. Talipov, B.T. Ibragimov, L.Yu. Izotova, Z.G. Tilyakov, D.N. Dalimov, Khim. Prir. Soedin. (Russ.) (2004) 422–424.
[43] P. Przybylski, K. Pyta, B. Wicher, M. Gdaniec, B. Brzezinski, J. Mol. Struct. 889 (2008) 332–343.
[44] J. Wouters, F.J. Luque, G.U. Barretta, F. Balzano, R. Pignatello, S. Guccione, J. Chem. Soc., Perkin Trans 2 (5) (2002) 1012–1016.
[45] S.J. Grabowski, J. Mol. Struct. TEOCHEM 811 (2007) 61–67.
[46] L. Sobczyk, S.J. Grabowski, T.M. Krygowski, Chem. Rev. 105 (2005) 3513–3560.
[47] A. Filarowski, A. Kochel, K. Cieslik, A. Koll, J. Phys. Org. Chem. 18 (2005) 986–993.
[48] Z. Rozwadowski, W. Schilf, B. Kamieński, Magn. Res. Chem. 43 (2005) 573–577.
[49] G. Zundel, J. Mol. Struct. 552 (2000) 81–86.
[50] P. Przybylski, B. Brzezinski, F. Bartl, Biopolymers 74 (2004) 273–286.
[51] F. Bohlmann, Chem. Ber. 91 (1958) 2157–2159.
[52] T. Masamune, M. Takasugi, M. Matsuki, Bull. Chem. Soc. Jpn. 41 (1968) 2466–2469.
[53] J. Konarski, J. Mol. Struct. 7 (1971) 337–354.
[54] B. Brycki, B. Brzezinski, B. Marciniak, S. Paszyc, Spectrosc. Lett. 24 (1991) 509–518.
[55] P. Przybylski, J. Kira, G. Schroeder, B. Brzezinski, F. Bartl, J. Phys. Chem. A 112 (2008) 8061–8069.
[56] W. Schilf, B. Kamienski, A. Szady-Chełmieniecka, E. Grech, A. Makal, K. Wozniak, J. Mol. Struct. 844–845 (2007) 94–101.
[57] T. Dziembowska, P.E. Hansen, Z. Rozwadowski, Prog. Nucl. Magn. Reson. Spectrosc. 45 (2004) 1–29.
[58] B.S. Siddiqui, S.T. Ali, M. Rasheed, M.N. Kardar, Helv. Chim. Acta 86 (2003) 2787–2796.
[59] D.H. O'Brien, R.D. Stipanovic, J. Org. Chem. 43 (1978) 1105–1111.
[60] C. Salas, V. Armstrong, C. Lopez, R.A. Tapia, Magn. Res. Chem. 46 (2008) 191–194.
[61] Z. Rozwadowski, J. Mol. Struct. 753 (2005) 127–135.
[62] J.D. Douglas, S.J. Senior, C. Morehouse, B. Phetsukiri, I.B. Campbell, G.S. Besra, D.E. Minnikin, Microbiology 148 (2002) 3101–3109.
[63] M.C.S. Lourenco, F.R. Vicente, M.d.G.M.d.O. Henriques, A.L. Peixoto Candea, R.S. Borges Goncalves, T.C.M. Nogueira, M. de Lima Ferreira, M.V. Nora de Souza, Bioorg. Med. Chem. Lett. 17 (2007) 6895–6898.
[64] L.N. Yuldasheva, A. Cruz e Carvalho, O.V. Krasilnikov, J. Incl. Phenom. Macrocycl. Chem. 60 (2008) 65–70.
[65] L.F.C. Medina, V. Stefani, A. Brandelli, Lett. Appl. Microbiol. 42 (2006) 381–385.
[66] R. Adams, R.C. Morris, T.A. Geissman, D.J. Butterbaugh, K.C. Kirkpatrick, J. Am. Chem. Soc. 60 (1938) 2193–2194.
[67] P. Przybylski, B. Brzezinski, F. Bartl, J. Mol. Struct. 794 (2006) 237–243.
[68] P. Przybylski, M. Małuszyńska, B. Brzezinski, J. Mol. Struct. 750 (2005) 152–157.
[69] G. Bejcar, P. Przybylski, M. Walkowiak, B. Brzezinski, J. Mol. Struct. 830 (2007) 72–77.
[70] G. Bejcar, P. Przybylski, J. Fusiara, B. Brzezinski, F. Bartl, J. Mol. Struct. 754 (2005) 31–36.
[71] G. Sheldrick, SHELXS-97, Program for Crystal Structure Solution, University of Goettingen, 1997.
[72] G. Sheldrick, SHELXL-97, Program for Crystal Structure Refinement, University of Goettingen, 1997.